Full and Independent Manipulation of Co- and Cross-polarized Waves with Metasurface

Jianxun Su [1], Jiayi Liu [1], Zengrui Li [1], and Lamar Y. Yang [2]

[1] School of Information and Communication Engineering
Communication University of China, Beijing, 100024, China
zrli@cuc.edu.cn

[2] Department of Electrical and Computer Engineering
University of Nebraska-Lincoln, NE, 68182, USA

Abstract — A novel metasurface based on the amplitude-phase manipulation and beamforming is proposed for the control of co- and cross-polarized wave simultaneously and independently. The metasurface consists of two polarization conversion elements (PCEs) and their mirrors: the two PCEs are used to control the co-polarized waves with the co-polarized field component of equal amplitude and opposite phase, and the mirrors of them that are intent to control the cross-polarized waves. Full manipulation of the amplitude and phase for both co- and cross-polarized components of the reflected waves is realized by adjusting the geometric parameters of two PCEs. Compared with the traditional co-polarized phase-only manipulation, freedom degree of manipulation is increased from 1 to 4, which greatly increases the ability of manipulating electromagnetic waves. The arrangement of PCEs is obtained based on the planar array theory to achieve the desired co-polarized and cross-polarized scattering patterns. The theoretical analysis, simulation and experiment results are in good agreement and verify the proposed mechanism.

Index Terms — Co-polarized, cross-polarized, metasurface, manipulation.

I. INTRODUCTION

As a very important breakthrough, metamaterials have powerful abilities to manipulate electromagnetic waves because they can be designed to have arbitrary permittivity and permeability. By tailoring the geometry or materials of the components, many special phenomena have been demonstrated, such as subwavelength imaging [1], beam rotation [2], invisibility cloaks [3, 4], and so on. Therefore, the use of ultra-thin design to effectively manipulate the propagation of electromagnetic waves attracted more and more research efforts. In recent years, the two-dimensional metamaterials which are called metasurfaces have subwavelength characteristics in the direction of wave propagation and greatly simplify the requirements of fabrication while maintaining powerful functionality of controlling the propagation properties of electromagnetic waves [5, 6]. By introducing abrupt phase discontinuities on the surface of the metal or dielectric structure, metasurfaces can realize extraordinary light manipulations, for example, light bending [7, 8], vortex beam generation [9], focusing [10, 11], wave plates [12, 13], holograms [14, 15], and microstrip filter [16]. Benefiting from small profile and flexible phase control, metasurfaces become very attractive and replace the traditional polarization controller for miniaturization devices. In the past few years, a variety of designs have been proposed to achieve effective polarization alteration from visible light to microwaves [17, 18]. Anisotropic structures such as T-shaped, C-shaped and L-shaped structures and the split ring are widely used to adjust the phase difference of two orthogonal electric field components [19, 20]. In addition to radar scattering cross section reduction, a new type of polarization conversion metasurface was put forward [21]. Theoretical and numerical of investigation of the chiral slab exhibiting polarization rotation is presented in detail [22].

Full control of both the magnitude and phase of transmission and reflection respectively are important issue for free manipulation of electromagnetic wave propagation. Recently, many efforts have been made to manipulate the electromagnetic waves by using metamaterials and metasurfaces. However, most of them mainly adjust the phase of the co-polarized component of the reflected waves, namely single-degree-of-freedom manipulation. For example, a method by designing the reflection-phase distributions of the anisotropic metasurface with Jerusalem Cross structures along the x and y directions has been proposed [23], the x- and y-polarized incident waves can be manipulated independently to realize multi-beam reflections. The proposed method provides an extensive approach to manipulate the reflected beams and their polarizations independently. Otherwise, methods to tailor the reflection

Submitted On: May 26, 2019
Accepted On: July 29, 2019

1054-4887 © ACES

and scattering of THz waves in an anomalous manner by using coding metamaterials have been presented [24-26]. The THz coding metamaterials realized by using two structures formed without and with, respectively, a metallic ring resonator on top of a metal ground plane in [24] are proposed. The anisotropic coding metasurfaces which use square-shaped and dumbbell-shaped metallic structures in [25] are proposed. A general coding unit based on a Minkowski closed-loop particle in [26] are proposed. The proposed structures have strong abilities to control THz waves by designing specific coding sequences of the phase of the co-polarized component of the reflected waves. These works reveal new methodology arising from coding metamaterials in effective manipulation of THz wave propagation and may offer widespread applications. In addition to effective medium parameters, the programmable metamaterials have recently been proposed as an alternative approach to manipulate the electromagnetic waves. The element integrated with one PIN diode is designed for two reflection-type elements with a 180° phase difference [27], and thus a binary coded phase is realized for a single polarization. Based on this idea, various functionalities, such as steering, bending, focusing and random electromagnetic waves scattering, can be simply implemented by digitally encoding metasurfaces with the corresponding coding sequences.

In this paper, we propose two metasurfaces based on a novel physical mechanism which can realize the beamforming and multi-degree-of-freedom manipulation of electromagnetic waves. We designed three different kinds of PCEs. By changing their geometric parameters, we can get the relationship between the amplitude and phase of the co-polarized and cross-polarized components of the reflected waves for different PCEs. By combining the proposed PCEs and their mirrors on the metasurface, we can realize the control of the amplitude and phase of the co- and cross-polarized components of the reflected waves, namely four-degree-of-freedom manipulation of electromagnetic waves. In this work, the state of the polarization mode and the power density distribution of the beams of the reflected waves can be manipulated flexibly and simultaneously. One of the metasurfaces is fabricated and measured to further prove the feasibility of our novel physical mechanism. The analysis, simulation and measurement results demonstrate that the proposed metasurface can realize beamforming and manipulate electromagnetic waves in four-degree-of-freedom, which may have potential applications in satellite communications, millimeter wave image system, radar system and so on.

II. THEORY AND PCE DESIGN

A. Theory

The design of coding sequences is based on the planar array theory. As shown in Fig. 1, "1" and "0" coding particles are distributed in a chessboard configuration. The lengths of each coding particle along x- and y-axis are marked by d_x and d_y, respectively. The planar array has N_x rows along the x axis and N_y columns along the y axis, $N_x = md_x$, $N_y = nd_y$.

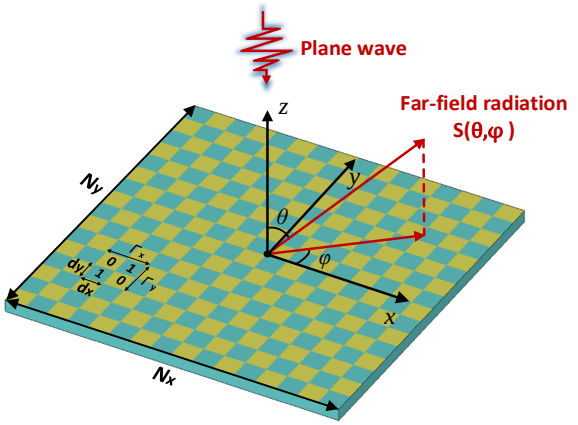

Fig. 1. The schematic for the rectangular grid coding plane array.

The formula for calculating the far-field pattern of the metasurface under the normal illumination of plane wave is expressed below:

$$S(\theta,\varphi)=\sum_{m=1}^{M}\sum_{n=1}^{N}R_{mn}\exp\{jk\sin\theta[(m-\frac{1}{2})d_x\cos\varphi+(n-\frac{1}{2})d_y\sin\varphi]\}, \tag{1}$$

where R_{mn} is the reflection coefficient of the (m, n)-th coding particle is defined by:

$$R_{mn}=A_{mn}e^{j\Psi_{mn}}=\begin{cases}Ae^{j\Psi_0} & \text{For coding particle "0",}\\ Ae^{j(\Psi_0+\pi)} & \text{For coding particle "1".}\end{cases} \tag{2}$$

For the 1-bit coding metasurface, the reflection amplitudes of coding particles "0" and "1" are unity and the phase difference between them are 0 and π, respectively. Since the absolute value of reflection phase Ψ_0 is a constant and can be moved out of the summation, it is assumed to be zero. The double summation in (1) can be separated as:

$$S(\theta,\varphi)=\sum_{m=1}^{M}\exp\{j[(m-\frac{1}{2})kd_x\sin\theta\cos\varphi+m\pi]\}\cdot\sum_{n=1}^{N}\exp\{j[(n-\frac{1}{2})kd_x\sin\theta\sin\varphi+n\pi]\}. \tag{3}$$

From (3) we can obtain the far field scattering of the reflected waves.

Next, the derivation of the abnormal reflection angle is introduced [25]. When the angles θ and φ satisfying the following conditions, the first diffraction order of the reflected beam becomes:

$$\varphi = \pm \arctan(\frac{d_x}{d_y}) \text{ and } \varphi = \pi \pm \arctan(\frac{d_x}{d_y}), \quad (4)$$

$$\theta = \arcsin(\frac{\pi}{k} \cdot \sqrt{\frac{1}{d_x^2} + \frac{1}{d_y^2}}) \cdot \quad (5)$$

Considering $\Gamma_x = 2d_x$, $\Gamma_y = 2d_y$, $k = 2\pi/\lambda$, (5) can be written as:

$$\theta = \arcsin(\lambda \cdot \sqrt{\frac{1}{\Gamma_x^2} + \frac{1}{\Gamma_y^2}}) \cdot \quad (6)$$

The anomalous reflection direction of the normally incident is given by (4) and (6). They are not only applicable to the coding metasurface encoded with 1-bit but also valid for higher bits. If the metasurface is encoded with periodic coding sequences along one direction (x- or y-direction), the elevation angle θ defined in equation can be simplified as below:

$$\theta = \arcsin(\frac{\lambda}{\Gamma}), \quad (7)$$

where λ and Γ represent the free-space wavelength and the physical length of one period of the coding sequence (that is the minimum length of gradient phase). So the anomalously deflected angles along the x- and y-directions can be independently calculated by (7).

B. PCE design

Electromagnetic waves controlled by PCEs are flexible and independent, and distinct functionalities can be realized via the combination of different elements and different arrangement. In order to ensure that the PCE is insensitive to the polarization of the impinging wave, the geometric structure is symmetrical with respect to 45° diagonal. For the sake of analysis, u- and v-axes are introduced here along 45° direction with respect to x- and y-directions. For the different power density distribution of the co- and cross-polarized components of the reflected waves, three types of PCEs have been presented, the structures of them are depicted in Fig. 2, and all of them are symmetrical along u- and v-axes. The PCEs are printed on the surface of PTFE woven glass (Model: F4B-2) substrate with a thickness of 2.93 mm and a dielectric constant ε_r = 2.65 (loss tangent tan δ = 0.001). As shown in Figs. 2 (a)-(c), PCE_1 is composed of a structure combined with a square ring and a cut wire, PCE_2 is a double-head arrow structure and PCE_3 is composed of a symmetric spilt ring and a cut wire. The geometric parameters of the structures are illustrated in Fig. 2. By changing the parameter values of the structures, two PCEs with equal amplitude and opposite phase in both co- and cross-polarized components at a certain frequency and their mirrors are selected. By designing coding sequences and forming a metasurface, the multi-degree-of-freedom manipulation of electromagnetic waves can be realized. The far-field scattering patterns are presented to demonstrate the characteristics of the encoded metasurface.

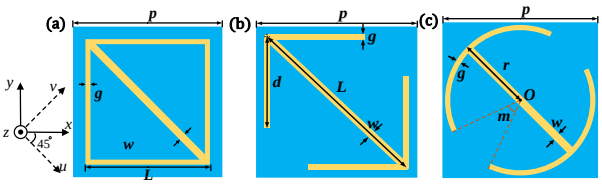

Fig. 2. The front view of the three PCEs: (a) PCE_1, p=6mm, g=0.2mm, w=0.3mm, L is a variable, (b) PCE_2, p=6mm, g=0.2mm, w=0.3mm, L is a variable, d=k*L (k=0.5), and (c) PCE_3, p=6mm, g=0.2mm, w=0.3mm, r=2.65mm, m is a variable.

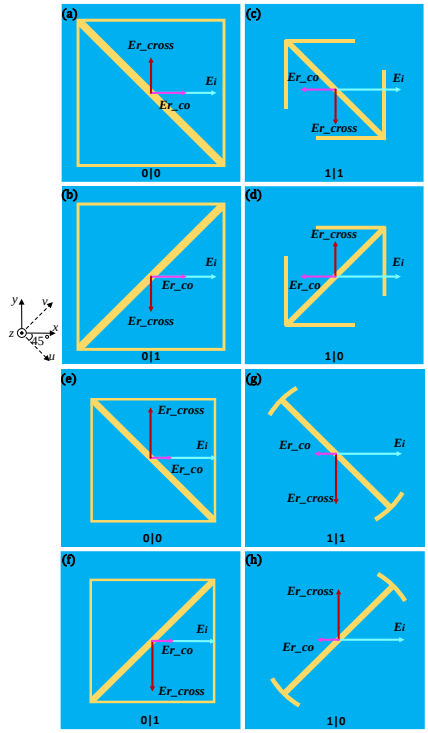

Fig. 3. The designed PCEs for the coding metasurfaces. The first group: (a) $PCE_{1\text{-}1}$, (b) the mirror of $PCE_{1\text{-}1}$, (c) $PCE_{2\text{-}1}$, and (d) the mirror of $PCE_{2\text{-}1}$. The second group: (e) $PCE_{1\text{-}2}$, (f) the mirror of $PCE_{1\text{-}2}$, (g) $PCE_{3\text{-}1}$, and (h) the mirror of $PCE_{3\text{-}1}$.

We use the 1-bit case to demonstrate the control of functionalities via the coding metasurface with PCEs. For the different power density distribution of the co- and cross-polarized components of the reflected waves, two groups of PCEs are picked out. The first group satisfies that both the co- and cross-polarized components of the reflected waves account for 50% of power density at 20.7 GHz. As shown in Figs. 3 (a)-(d), it consists of four PCEs: PCE_1 with L=5.1 mm which is marked as $PCE_{1\text{-}1}$, PCE_2 with L=3.15 mm which is marked as $PCE_{2\text{-}1}$ and their mirrors. The numerical simulation results of the reflected amplitude and phase obtained by CST indicate that $PCE_{1\text{-}1}$ and $PCE_{2\text{-}1}$ have equal

amplitude and nearly 180° phase difference in both co- and cross-polarized components of the reflected waves at 20.7 GHz under the normal x-polarized incident waves as shown in Fig. 4. For $PCE_{1\text{-}1}$, the amplitude and phase of co-polarized reflected waves are 0.71 and 453.3°, the amplitude and phase of cross-polarized reflected waves are 0.70 and -543.6°. For $PCE_{2\text{-}1}$, the amplitude and phase of co-polarized reflected waves are 0.71 and -273.2°, and the amplitude and phase of cross-polarized reflected waves are 0.70 and -363.1°.

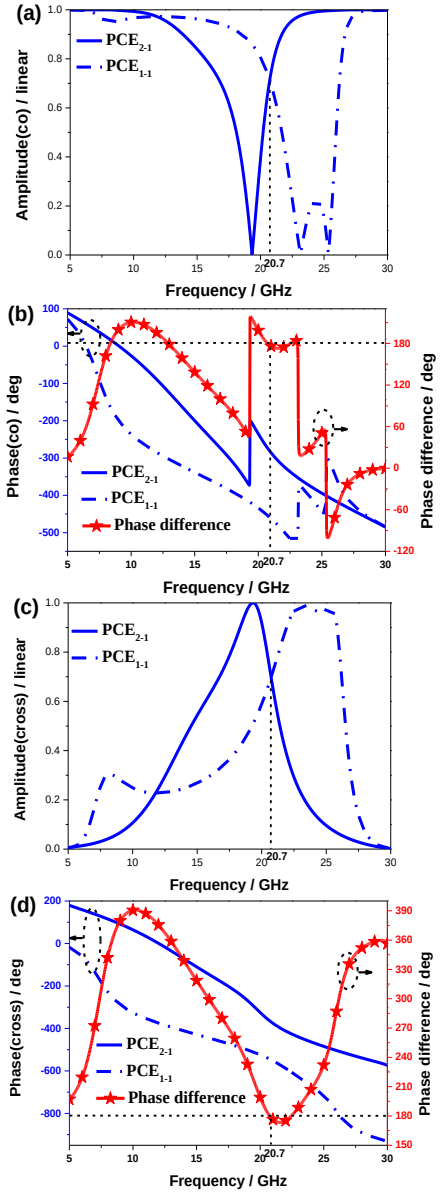

Fig. 4. The co- and cross-polarized reflection coefficients for $PCE_{1\text{-}1}$ and $PCE_{2\text{-}1}$ under normal x-polarized incident waves: (a) amplitude and (b) phase of co-polarized reflection coefficient, (c) amplitude and (d) phase of cross-polarized reflection coefficient.

Besides, the co-polarized components of the reflected waves of the PCE and their mirrors are equal in amplitude and phase, while the cross-polarized components of reflected waves are equal in amplitude but opposite in phase. The combination of the four PCEs can realize the control of co- and cross-polarized.

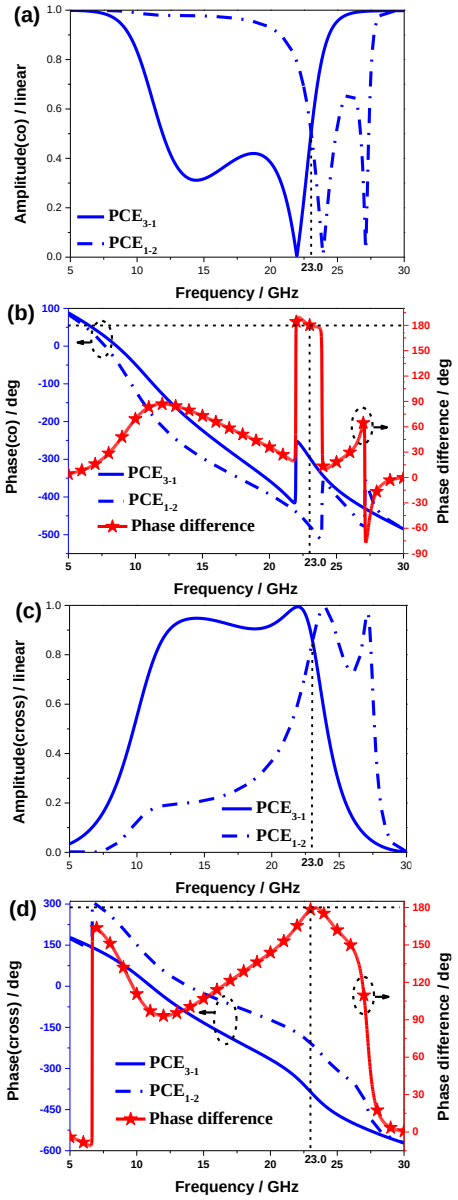

Fig. 5. The co- and cross-polarized reflection coefficients for $PCE_{1\text{-}2}$ and $PCE_{3\text{-}1}$ under normal x-polarized incident waves: (a) amplitude and (b) phase of co-polarized reflection coefficient, (c) amplitude and (d) phase of cross-polarized reflection coefficient.

The second group satisfies that the co-polarized component of the reflected waves accounts for 25% of power density at 23.0 GHz and the cross-polarized

component accounts for 75%. As shown in Figs. 3 (e)-(h), it consists of four elements: PCE_1 with L=4.15 mm which is marked as $PCE_{1\text{-}2}$, PCE_3 with m=151° which is marked as $PCE_{3\text{-}1}$ and their mirrors. The numerical simulation results of the reflected amplitude and phase indicate that $PCE_{1\text{-}2}$ and $PCE_{3\text{-}1}$ have equal amplitude and nearly 180° phase difference in both co- and cross-polarized components of the reflected waves at 23.0 GHz under the normal x-polarized incident waves as shown in Fig. 5. For $PCE_{1\text{-}2}$, the amplitude and phase of co-polarized reflected waves are 0.51 and -476.9°, and the amplitude and phase of cross-polarized reflected waves are 0.85 and -207.7°. For $PCE_{3\text{-}1}$, the amplitude and phase of co-polarized reflected waves are 0.50 and -297.0°. The amplitude and phase of cross-polarized reflected waves are 0.86 and -386.3°.

III. DESIGN, SIMULATION, AND MEASUREMENT OF METASURFACES

A. Design and simulation of metasurfaces

The elements mentioned above (Fig. 3) are defined as '0|0' '1|0' '0|1' '1|1' coding particles, where the binary codes before and after the symbol (|) represent the digital states of co- and cross-polarized components of reflected waves, respectively. The selection and arrangement of PCEs on the metasurface requires two steps. For example, we use $PCE_{1\text{-}1}$ and $PCE_{2\text{-}1}$ and their mirrors to design a metasurface. The first step is to determine the coding table for the co-polarized component. Because $PCE_{1\text{-}1}$ and the mirror of $PCE_{2\text{-}1}$ have equal amplitude and opposite phase in co-polarized component of the reflected waves at 20.7 GHz under the normal x-polarized incident waves, they are used to design the desired co-polarized scattering pattern based on array theory [28]. Secondly, the coding table for the desired cross-polarized scattering pattern is also determined based on planar array theory. If it has the same code with co-polarized component at the same location, the PCE at that location doesn't change, however, the PCE should be changed to its mirror. The process for the arrangement of PCEs on the metasurface is shown in the Fig. 6.

In order to further analyze the coding metamaterials quantitatively, we first use $PCE_{1\text{-}1}$, $PCE_{2\text{-}1}$ and their mirrors to encode a metasurface MS_1. MS_1 is formed by repeating a 2D code matrix m_1 with a simple coding sequence of '010101…' along x-axis for the digital states of co-polarized component of reflected waves as well as '010101…' alternates with '101010…' along y-axis for the digital states of cross-polarized component:

$$m_1 = \begin{bmatrix} 0|1 & 1|0 \\ 0|0 & 1|1 \end{bmatrix}.$$

The lattice as shown in Fig. 7 (a) generated by a subarray of the same basic PCEs with a size of 5×5, is used to minimize the unwanted coupling effect resulting from adjacent elements with different geometries. The final encoded metasurface MS_1 that contains 6×6 lattices (Fig. 7 (a)) is designed to illustrate the novel physical mechanism. We apply the open boundary condition and plane wave excitation in CST Microwave Studio to simulate the whole encoded metasurface MS_1. Figures 8 (a)-(c) shows the total, co-polarized and cross-polarized 3D far-field scattering patterns of MS_1 under the normal x-polarized incident waves at 20.7 GHz. The co-polarized component of reflected waves is equally split into two symmetrically oriented beams in the x-z plane at the same angle with respect to z-axis as shown in Fig. 8 (b). And the cross-polarized component of reflected waves is equally split into four symmetrically oriented beams in the φ=45° and 135° planes at the same angle with respect to the z-axis as shown in Fig. 8 (c). In theory, if the co- and cross-polarized components of the reflected waves account for 50% of power density respectively, the power density of each of four beams of cross-polarized component should be decreased by 3.01 dBm^2 compared to each of two beams of co-polarized component. In the result of our simulation, the power density of each of four beams of cross-polarized component is 7.30 dBm^2 while each of two beams of co-polarized component is 10.80 dBm^2, and the difference between them is 3.50 dBm^2, basically consistent with the theoretical value. Besides, the anomalous reflection angle can be calculated by (5) and (6) theoretically. For the main two beams of co-polarized of reflected waves, θ is 13.96°. And for the main four beams of cross-polarized component of reflected waves, θ is 19.95°. The simulated results demonstrate that the main lobe of co-polarized component in the x-z plane deviates from the z-axis to 13.5°, and the main lobe of cross-component in the φ=45° and 135° planes deviates from the z-axis to 19.3°. So the simulation result of the anomalous reflection angle agrees well with the analytical predictions. The 2D far-field scattering pattern in the x-z plane for co-polarized component is shown in Fig. 9 (a), and the patterns in the φ=45°and 135° planes for cross-polarized component are shown in Figs. 9 (b)-(c). We consider that the small disturbance observed in the scattered electric field is attributed to the true reflection phase difference of the adjacent lattice coupling, which is not exactly 180° at 20.7 GHz. However, if we increase the size of the lattice, this effect can be suppressed.

Based on the designed method of MS_1, we further propose coding metasurface MS_2 as shown in Fig. 7 (b) which consists of $PCE_{1\text{-}2}$, $PCE_{3\text{-}1}$ and their mirrors. The coding sequences of MS_2 are '101010' alternates with '010101…' along x-axis for the digital states of co-polarized component and a random matrix [25] for the digital states of cross-polarized component of reflected waves. The coding matrix is written as:

$$m_2 = \begin{bmatrix} 0|1 & 1|1 & 0|0 & 1|1 & 0|0 & 1|0 & 0|1 & 1|1 \\ 1|1 & 0|1 & 1|1 & 0|1 & 1|0 & 0|0 & 1|1 & 0|0 \\ 0|0 & 1|0 & 0|1 & 1|1 & 0|0 & 1|1 & 0|0 & 1|1 \\ 1|1 & 0|1 & 1|1 & 0|0 & 1|1 & 0|1 & 1|1 & 0|0 \\ 0|1 & 1|1 & 0|1 & 1|1 & 0|1 & 1|0 & 0|1 & 1|1 \\ 1|0 & 0|0 & 1|0 & 0|0 & 1|0 & 0|0 & 1|0 & 0|0 \\ 0|0 & 1|1 & 0|1 & 1|1 & 0|1 & 1|0 & 0|0 & 1|1 \\ 1|1 & 0|0 & 1|1 & 0|0 & 1|0 & 0|1 & 1|0 & 0|1 \end{bmatrix}.$$

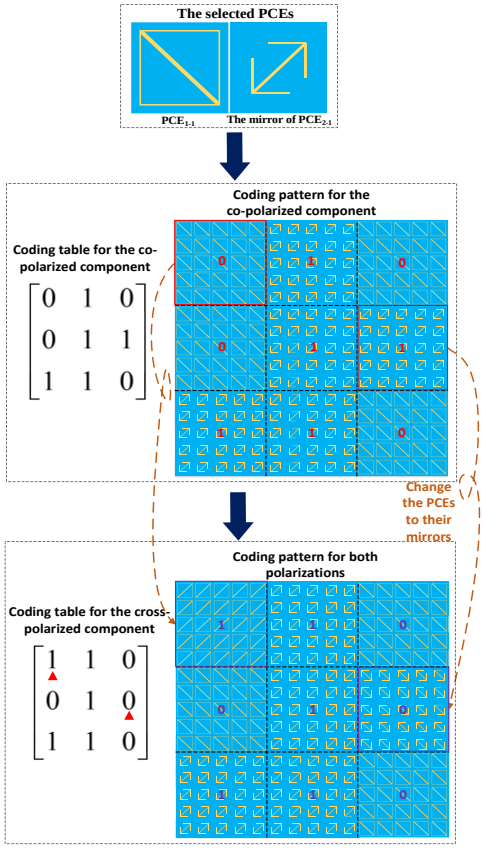

Fig. 6. The process for the arrangement of PCEs on the metasurface.

The basic PCEs of MS_2 are $PCE_{1\text{-}2}$, $PCE_{3\text{-}1}$ and their mirrors. MS_2 satisfies that the co-polarized component of the reflected waves accounts for 25% of power density at 23.0 GHz and the cross-polarized component accounts for 75%. Figures 8 (d)-(f) shows the total, co-polarized and cross-polarized 3D far-field scattering patterns of MS_2 under the normal x-polarized incident waves at 23.0 GHz. The co-polarized component of reflected waves which accounts for 25% of power density is equally split into four symmetrically oriented beams in the φ=45° and 135° planes at the same angle with respect to the z-axis as shown in Fig. 8 (e). And the cross-polarized component of reflected waves is randomly scattered into many directions and results in a diffusion pattern in the upper half- space which is shown in Fig. 8 (f).

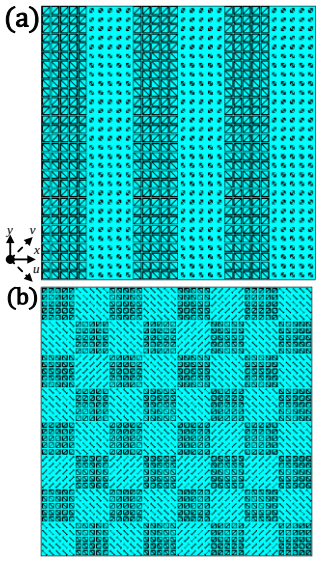

Fig. 7. Coding patterns of two 1-bit metasurfaces: (a) Pattern of MS_1 that contains 6×6 lattices with a size of 5×5, and (b) pattern of MS_2 that contains 8×8 lattices with a size of 5×5.

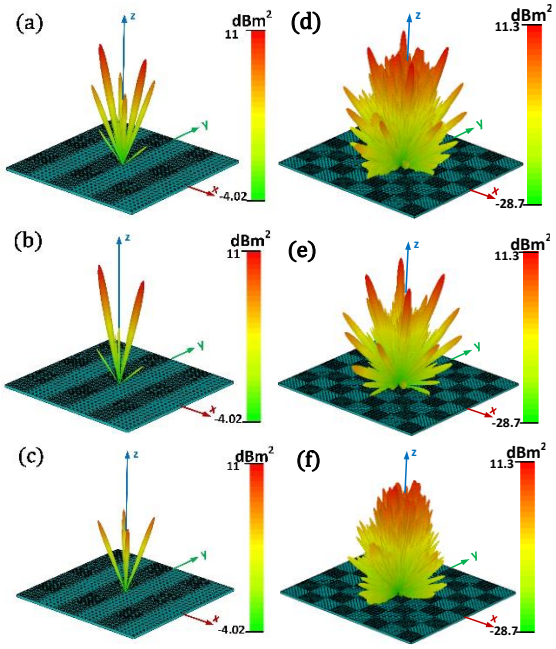

Fig. 8. Simulated 3D far-field scattering patterns for two metasurfaces under the normal x-polarized incident waves: (a)-(c) The total, co-polarized and cross-polarized 3D far-field scattering patterns of MS_1 at 20.7 GHz, and (d)-(f) the total, co-polarized and cross-polarized 3D far-field scattering patterns of MS_2 at 23.0 GHz.

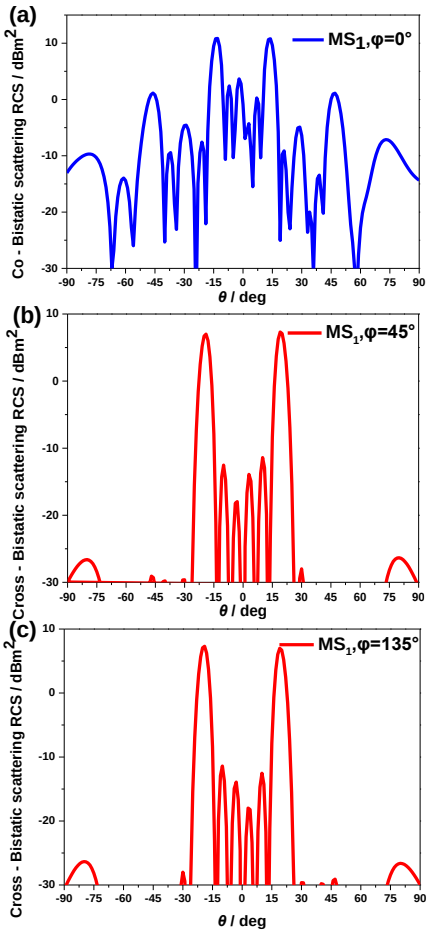

Fig. 9. Simulated 2D far-field scattering patterns for MS_1 under the normal x-polarized incident waves at 20.7 GHz: (a) The co-polarized 2D far-field scattering patterns of MS_1 in the x-z plane, and (b)-(c) the cross-polarized 2D far-field scattering patterns of MS_1 in φ=45° and 135° plane.

B. Measurement of the metasurface

To further verify the design, a sample (300 mm x 300 mm) of the metasurface is fabricated, as depicted in Fig. 10 (a), which is an extension of MS_1. The sample is manufactured by LPKF ProtoLaser using printed circuit board (PCB) technology. The dielectric substrate is F4B-2 substrate with a thickness of 2.93 mm and a dielectric constant ε_r = 2.65 (loss tangent tan δ = 0.001). The metal patches and ground are 0.035 mm-thick copper layers. For bistatic measurement setup shown in Fig. 10 (b), transmit antenna is fixed while receive antenna moves along an arc track to detect the reflection fields at scattering angle θ from 6° to 90°. Because the two antennas are very close to each other in the range of -6° to 6°, the bistatic measurement setup is similar to a monostatic measurement setup. Therefore, accurate measurement results cannot be obtained at these locations. Measurement results of bistatic RCS along the principal (XoZ) plane for the metasurface are presented in Fig. 11, which is the co-polarized 2D far-field scattering pattern of the sample under the normal x-polarized incident waves at 20.7 GHz. It shows that the measured results agree well with the simulations especially the main lobes and verifies that the proposed metasurface can realize the beamforming and multi-degree-of-freedom manipulation of electromagnetic waves. And we consider that the small perturbations observed in the scattered electric field are caused by the true reflection phase difference of the coupling of adjacent lattices.

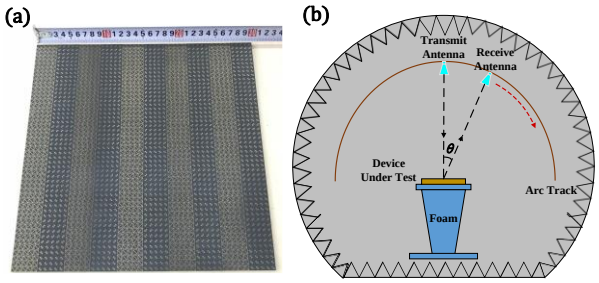

Fig. 10. Photographs of the fabricated sample and schematics of the experimental setup: (a) a sample which is an extension of MS_1, and (b) measurement setup for bistatic RCS.

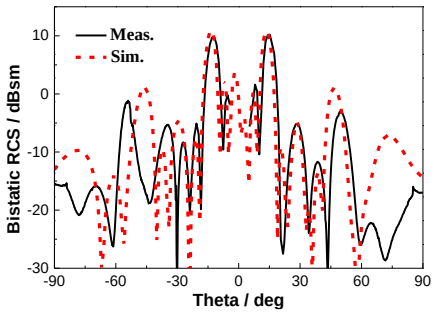

Fig. 11. The measured co-polarized bistatic RCS of the sample under the normal x-polarized incident waves at 20.7 GHz.

IV. CONCLUSION

We have proposed two anisotropic metasurfaces based on a novel mechanism to control the co- and cross-polarized waves full and independently, thus the beamforming and the multi-degree-of-freedom manipulation of electromagnetic waves have been realized. The metasurface, which can increase the freedom degree of manipulation from 1 to 4 compared with co-polarized phase-only manipulation, is composed of two types of PCEs and their mirrors. The full-wave simulated results verify that the scattering pattern of co- and cross-polarized waves can be manipulated independently and simultaneously, such as beamforming,

scattering angles and polarization states. To validate the proposed design, one typical metasurface has been fabricated and measured. Our experiment results show very good agreement with the corresponding simulation in terms of bistatic RCS pattern. In addition, the flexibility in manipulating the electromagnetic waves can be provided by selecting more kinds of combinations of PCEs and diversifying the arrangement of them on metasurfaces. The proposed metasurface shows the advantage of easy fabrication, compactness, and also provides a good choice for manipulating the reflected beams and their polarizations independently, which makes it promising in the broad applications such as electromagnetic cloaking, subwavelength imaging, beam rotation, etc.

ACKNOWLEDGMENT

This work was supported by the National Natural Science Foundation of China (NSFC) under Grant No. 61671415, No. 61701448 and No. 61331002, and the Fundamental Research Fund for the Central Universities under grant No. CUC19ZD001.

REFERENCES

[1] J. B. Pendry, "Negative refractive makes a perfect lens," *Phys. Rev. Lett.*, vol. 85, pp. 3966-3969, 2000.

[2] H. Chen, B. Hou, S. Chen, X. Ao, W. Wen, and C. T. Chan, "Design and experimental realization of a broadband transformation media field rotator at microwave frequencies," *Phys. Rev. Lett.*, vol. 102, p. 183903, 2009.

[3] J. B. Pendry, D. Schurig, and D. R. Smith, "Controlling electromagnetic fields," *Science*, vol. 312, pp. 1780-1782, 2006.

[4] D. Schurig, J. J. Mock, B. J. Justice, et al., "Metamaterial electromagnetic cloak at microwave frequencies," *Science*, vol. 314, pp. 977-980, 2006.

[5] S. Y. Luo, Y. S. Li, Y. F. Xia, and L. Zhang, "A low mutual coupling antenna array with gain enhancement using metamaterial loading and neutralization line structure," *Appl. Comput. Electromagn. Soc. J.*, vol. 34, pp. 411-418, 2019.

[6] K. Yu, Y. S. Li, and X. G. Liu, "Mutual coupling reduction of a MIMO antenna array using 3-D novel meta-material structures," *Appl. Comput. Electromagn. Soc. J.*, vol. 33, 2018.

[7] N. Yu, P. Genevet, M. A. Kats, et al., "Light propagation with phase discontinuities reflection and refraction," *Science*, vol. 334, pp. 333-337, 2011.

[8] X. Ni, N. K. Emani, A. V. Kildishev, et al., "Broadband light bending with plasmonic nano-antennas," *Science*, vol. 335, p. 427, 2012.

[9] L. Huang, X. Chen, H. Mühlenbernd, et al., "Dispersionless phase discontinuities for controlling light propagation," *Nano Lett.*, vol. 12, pp. 5750-5755, 2012.

[10] F. Aieta, P. Genevet, M. A. Kats, et al., "Aberration-free ultrathin flat lenses and axicons at telecom wavelengths based on plasmonic metasurfaces," *Nano Lett.*, vol. 12, pp. 4932-4936, 2012.

[11] A. Pors, M. G. Nielsen, R. L. Eriksen, et al., "Broadband focusing flat mirrors based on plasmonic gradient metasurfaces," *Nano Lett.*, vol. 13, pp. 829-834, 2013.

[12] Y. Yang, W. Wang, P. Moitra, et al., "Dielectric meta-reflectarray for broadband linear polarization conversion and optical vortex generation," *Nano Lett.*, vol. 14, pp. 1394-1399, 2014.

[13] N. Yu, F. Aieta, P. Genevet, et al., "A broadband, background-free quarter-wave plate based on plasmonic metasurfaces," *Nano Lett.*, vol. 12, pp. 6328-6333, 2012.

[14] X. Ni, A. V. Kildishev, and V. M. Shalaev, "Metasurface holograms for visible light," *Nat. Commun.*, vol. 4, 2013.

[15] L. Huang, X. Chen, H. Mühlenbernd, et al., "Three-dimensional optical holography using a plasmonic metasurface," *Nat. Commun.*, vol. 4, pp. 2808, 2013.

[16] M. A. Abaga Abessolo, Y. Diallo, A. Jaoujal, A. E. I. Moussaoui, and N. Aknin, "Stop-band filter using a new metamaterial complementary split triangle resonators (CSTRs)," *Appl. Comput. Electromagn. Soc. J.*, vol. 28, pp. 353-358, 2013.

[17] F. Ding, Z. Wang, S. He, et al., "Broadband high-efficiency half-wave plate: A super-cell based plasmonic metasurface approach," *ACS Nano.*, vol. 9, pp. 4111-4119, 2015.

[18] A. Shaltout, J. Liu, V. M. Shalaev, et al., "Optically active metasurface with non-chiral plasmonic nano-antennas," *Nano Lett.*, vol. 14, pp. 4426-4431, 2014.

[19] S. C. Jiang, X. Xiong, Y. S. Hu, et al., "High-efficiency generation of circularly polarized light via symmetry-induced anomalous reflection," *Phys. Rev. B.*, vol. 91, 2015.

[20] S. C. Jiang, X. Xiong, Y. S. Hu, et al., "Controlling the polarization state of light with a dispersion-free metastructure," *Phys. Rev. X.*, vol. 4, 2014.

[21] J. X. Su, C. Y. Kong, Z. R. Li, X. J. Yuan, and Y. Q. Yang, "Ultra-wideband and polarization-insensitive RCS reduction of microstrip antenna using polarization conversion metasurface," *Appl. Comput. Electromagn. Soc. J.*, vol. 32, pp. 524-530, 2017.

[22] I. Comez, M. Kraaslan, F. Dincer, F. Karadag, and C. Sabah, "Systematic analysis on the optical

properties of chiral metamaterial slab for microwave polarization control," *Appl. Comput. Electromagn. Soc. J.*, vol. 30, pp. 478-487, 2015.
[23] F. M. Hui, Q. L. Yan, and L. Kang, "Multi-beam reflections with flexible control of polarizations by using anisotropic metasurfaces," *Sci. Rep.*, vol. 6, 2016.
[24] L. Liang, M. Qi, J. Yang, et al., "Anomalous terahertz reflection and scattering by flexible and conformal coding metamaterials," *Adv. Opt. Mater.*, vol. 3, pp. 1374-1380, 2015.
[25] S. Liu, T. J. Cui, Q. Xu, et al., "Anisotropic coding metamaterials and their powerful manipulation of differently polarized terahertz waves," *Light Sci. Appl.*, vol. 5, 2016.
[26] L. H. Gao, Q. Cheng, J. Yang, et al., "Broadband diffusion of terahertz waves by multi-bit coding metasurfaces," *Light Sci. Appl.*, vol. 4, 2015.
[27] H. Yang, X. Cao, Y. Fan, et al., "A programmable metasurface with dynamic polarization, scattering and focusing control," *Sci. Rep.*, vol. 6, 2016.
[28] C. A. Balanis, *Antenna Theory: Analysis and Design*. 3rd Edition, Wiley, New York, 2005.

Jianxun Su received the B.S. degree in Electronic Information Engineering from Taiyuan University of Technology, Taiyuan, China, in 2006; the M.S. degree and the Ph.D. degree in Electromagnetic Field and Microwave Technology from the Communication University of China and Beijing Institute of Technology, Beijing, China, in 2008 and 2011, respectively.

From 2012 to 2014, he was with China Electronics Technology Group Corporation (CETC), where he engaged in phased-array system research. He is currently working as associate researcher at School of Information Engineering, Communication University of China and also with the Science and Technology on Electromagnetic Scattering Laboratory. His special research interests include integral equation method, metamaterial, phased-array antenna, radar target characteristics.

Jiayi Liu received the B. Eng. degree in Communication Engineering from the Communication University of China in 2017. She is currently pursuing the M.S. degree at Communication University of China.

Her research interests include metamaterial, corner reflector and electromagnetic wave manipulation.

Zengrui Li received the B.S. degree in Communication and Information System from Beijing Jiaotong University, Beijing, China, in 1984; the M.S. degree in Electrical Engineering from Beijing Broadcast Institute, Beijing, China, in 1987; and the Ph.D. degree in Electrical Engineering from Beijing Jiaotong University, Beijing, China, in 2009.

He is currently a Professor with the Communication University of China, Beijing, China. He studied at Yokohama National University, Yokohama, Japan, from 2004 to 2005. His research interests include the areas of finite-difference time-domain (FDTD) methods, electromagnetic scattering, metamaterials and antennas. Li is a Senior Member of the Chinese Institute of Electronics.

Yaoqing Lamar Yang (S'02-M'09-SM'09) received his B.S. degree from the Northern Jiaotong University, China, in 1983, and his M.S. degree from the Beijing Broadcast Institute, China, in 1986, both in Electrical Engineering. He received his Ph.D. degree in the area of Wireless Communications and Networks from the University of Texas (UT) at Austin in 2006. He is now an Associate Professor in the Department of Computer and Electronics Engineering, University of Nebraska-Lincoln (UNL).

His current research interests lie in wireless communications and networks with emphasis on radio channel characterizations, cognitive radio networks, and statistical signal processing. Yang is a senior member of IEEE.